

Unveiling a Novel Metal-to-Metal Transition in LuH₂: Critically Challenging Superconductivity Claims in Lutetium Hydrides

Dong Wang¹, Ningning Wang², Caoshun Zhang¹, Chunsheng Xia¹, Weicheng Guo¹, Xia Yin¹, Kejun Bu¹, Takeshi Nakagawa¹, Jianbo Zhang¹, Federico Gorelli¹, Philip Dalladay-Simpson¹, Thomas Meier¹, Xujie Lü¹, Liling Sun^{1,2}, Jinguang Cheng², Qiaoshi Zeng¹, Yang Ding^{1*} and Ho-kwang Mao^{1,3}

¹ *Center for High-Pressure Science and Technology Advanced Research, Beijing, 100094, China*

² *Beijing National Laboratory for Condensed Matter Physics and Institute of Physics, Chinese Academy of Sciences, Beijing 100190, China*

³ *Shanghai Key Laboratory of Material Frontiers Research in Extreme Environments (MFree), Shanghai Advanced Research in Physical Sciences (SHARPS), Shanghai 201203, China*

**Correspondence: yang.ding@hpstar.ac.cn*

Following the recent report by Dasenbrock-Gammon et al. (2023) of near-ambient superconductivity in nitrogen-doped lutetium trihydride (LuH_{3-δ}N_ε), significant debate has emerged surrounding the composition and interpretation of the observed sharp resistance drop. Here, we meticulously revisit these claims through comprehensive characterization and investigations. We definitively identify the reported material as lutetium dihydride (LuH₂), resolving the ambiguity surrounding its composition. Under similar conditions (270-295 K and 1-2 GPa), we replicate the reported sharp decrease in electrical resistance with a 30% success rate, aligning with Dasenbrock-Gammon et al.'s observations. However, our extensive investigations reveal this phenomenon to be a novel, pressure-induced metal-to-metal transition intrinsic to LuH₂, distinct from superconductivity. Intriguingly, nitrogen doping exerts minimal impact on this transition. Our work not only elucidates the fundamental properties of LuH₂ and LuH₃ but also critically challenges the notion of superconductivity in these lutetium hydride systems. These findings pave the way for future research on lutetium hydride systems while emphasizing the crucial importance of rigorous verification in claims of ambient temperature superconductivity.

The 1911 discovery of superconductivity in mercury at 4.2 K, characterized by its vanishing electrical resistance, sparked a pivotal chapter in condensed matter physics¹. This ignited an ongoing quest for materials exhibiting higher transition temperatures (T_c), a crucial factor for potential breakthroughs in critical technologies like energy transmission and transportation. The subsequent emergence of cuprates^{2,3}, boasting T_c surpassing liquid nitrogen's boiling point (77.4 K), represented a significant leap forward. More recently, certain hydrides have also gained attention for displaying superconductivity above 200 K, albeit under extreme pressures exceeding 100 GPa⁴⁻¹⁰.

In 2023, a particularly captivating yet controversial claim captured global attention. Dasenbrock-Gammon et al. reported the tantalizing observation of potential near-room-temperature superconductivity in a lutetium-hydrogen-nitrogen (Lu-H-N) compound at 294 K under modest pressure (1 GPa)¹¹. However, the paper has since been retracted due to concerns about the reliability of the electrical resistance data and its analysis¹². Consequently, the finding remains shrouded in uncertainty, with lingering questions surrounding the exact composition of the compound and the true nature of the observed decrease in electrical resistance. Further experimental verification and a deeper understanding of the underlying mechanisms are crucial to elucidating whether this preliminary study genuinely achieves the long-sought goal of ambient temperature superconductivity.

A significant controversy surrounds the composition of the proposed Lu-N-H compound. Dasenbrock-Gammon et al. propose that this phase is nitrogen-doped trihydride $\text{LuH}_{3-\delta}\text{N}$, attributing it to the observed blue-to-pink color transition and superconductivity. However, their claim contradicts established knowledge, which associates such color changes with the face-cubic-center (fcc) phase present in dihydride LuH_2 ¹³⁻²¹. While theoretical models suggest the possibility of nitrogen-doped fcc LuH_3 mimicking LuH_2 ²²⁻²⁹, experimental evidence demonstrates that LuH_3 maintains its trigonal symmetry at pressures below 10 GPa³⁰. Unfortunately, challenges in accurately quantifying hydrogen content hinder researchers' efforts to accurately determine the composition of the reported superconducting phase.

More importantly, the claimed near-ambient superconductivity of $\text{LuH}_{3-\delta}\text{N}_\delta$ at 294 K and 1 GPa remains unconfirmed by independent studies, casting doubt on its reality. Despite claims of a 35% replication success rate, subsequent investigations have failed to replicate these findings^{13-18,31-34}. While some studies have observed a similar drop in electrical resistance, alternative explanations, including metal-insulator transitions³² or percolative phenomena³⁴, have been proposed. This controversy highlights the crucial need for meticulous compositional analysis and rigorous validation before accepting any claim of superconductivity in this material.

To comprehensively investigate the controversial findings of Dasenbrock-Gammon et al., we meticulously replicated their synthesis protocol, exposing high-purity lutetium foil to a precisely calibrated 99:1 $\text{H}_2:\text{N}_2$ gas mixture under identical conditions of 2 GPa, 65 °C, and 24 hours¹¹. Recognizing the inherent difficulty in differentiating between fcc LuH_2 and LuH_3 phases, we employed a separate strategy: synthesizing nitrogen-doped variants of both materials. We independently treated both LuH_2 and LuH_3 with nitrogen gas at 2 GPa for varying durations (1-5 days) at an elevated temperature of 200 °C to enhance the reaction kinetics. This approach enabled

independent investigations of each material's properties, culminating in a comprehensive comparative analysis that clearly distinguished their unique characteristics.

Our comprehensive investigation, employing a combination of advanced analytical techniques including optical microscopy, X-ray diffraction, Raman spectroscopy, and electrical resistance measurements³⁵, yielded results significantly divergent from those of Dasenbrock-Gammon et al.¹¹. We observed that lutetium metal remains largely unchanged under the prescribed H₂:N₂ gas mixture conditions of 2 GPa, 65 °C, and 24 hours¹¹. Importantly, nitrogen-doped LuH₃ retained its insulating, grey, and trigonal characteristics even under pressures exceeding 10 GPa. These findings offer compelling evidence that both the fcc metallic phase and the blue-to-pink color changes previously attributed to LuH_{3-δ}N_ε are inherent to LuH₂.

Crucially, electrical resistance measurements on both nitrogen-doped and undoped LuH₂ samples revealed a significant drop at 270-295 K and 1-2 GPa, with a success rate of 30%, consistent with observations by Dasenbrock-Gammon et al. However, our further experiments indicate that this reduction corresponds to a metal-to-metal phase transition rather than superconductivity. Consequently, we assert that the observed decrease in electrical resistance is more accurately attributed to a metal-to-metal transition in LuH₂, rather than indicative of superconductivity in LuH_{3-δ}N_ε. Further details are provided in the subsequent sections.

Reproducibility of the Published Protocol

Figures 1a and 1b illustrate characterization results obtained by meticulously adhering to the original synthesis protocol outlined by Dasenbrock-Gammon et al. Unexpectedly, lutetium metal chips approximately seven microns thick retain their original color even when exposed to a 99:1 H₂:N₂ gas mixture at pressures exceeding 3.0 GPa.

X-ray diffraction (XRD) analyses, presented in Figure 1d, reveal the dominant presence of unreacted lutetium metal, contradicting the anticipated formation of a blue, nitrogen-doped lutetium hydride phase. Additionally, high-pressure electrical resistance profiles, shown in Figures 1e and 1f, exhibit a typical metallic behavior characterized by linear temperature dependence above 50 K, thus challenging prior claims of superconducting phase transitions in nitrogen-doped lutetium hydrides.

Recent studies suggest that extending the reaction time³² or employing thinner lutetium metal foils³³ promotes the formation of lutetium hydrides, highlighting the slow kinetics of the reaction at these pressure-temperature conditions.

Color and Structure of Nitrogen-Doped LuH₃

LuH₃ exhibits trigonal symmetry under ambient conditions and transitions to a cubic phase above 10 GPa³⁰. While Dasenbrock-Gammon et al. proposed that trace nitrogen might stabilize this cubic metallic LuH₃ phase below 2 GPa and 65 °C, this proposition has not yet been experimentally confirmed.

To investigate this, we conducted experiments exposing LuH₃ to N₂ gas for 24 hours at 2.0 GPa and 200.0 °C (Fig. 2a). Notably, the temperature was elevated by 135 °C compared to the 65 °C used by Dasenbrock-Gammon et al. to further enhance reaction kinetics. Even at elevated

pressures exceeding 30.2 GPa, the intrinsic dark grey hue of LuH₃ remains unchanged (Fig. 2b and S1). XRD and Raman spectroscopic analyses (Fig. 2c and 2d) corroborate that the crystalline lattice largely retains its initial trigonal symmetry after heat treatment at 2 GPa. Furthermore, the electrical resistance of nitrogen-doped LuH₃ remains within a consistent range of 10⁵ - 10⁷ Ohm (Ω) up to pressures approaching 9.3 GPa (Fig. 2e and 2f), reinforcing its intrinsic insulating behavior. Increasing the reaction time between LuH₃ and N₂ gas to 5 days did not lead to any noticeable changes.

These data collectively cast doubt on the hypothesis that trace nitrogen quantities could stabilize a metallic fcc LuH_{3-δ}N_ε phase, which was purported to undergo a color change from blue to pink at pressures exceeding 0.3 GPa¹¹.

Composition of Reported Compound: LuH₃ or LuH₂

Figure 3 explores the influence of nitrogen on LuH₂ under consistent experimental conditions. Notably, the pressurized nitrogen-doped LuH₂ exhibits a striking color change from blue to pink or red (Fig. 3a and S2). Single-crystal XRD and Raman spectroscopy (Fig. 3b and 3c) confirm the stabilization of this phase into a fcc structure. This fcc structure exhibits a lattice parameter of 5.0378 Å, compared to the pristine LuH₂ sample's 5.0235 Å. This lattice expansion suggests the incorporation of nitrogen atoms into the crystal lattice. In addition, electrical resistance measurements (Fig. 3d) reveal a conventional metallic state in nitrogen-doped LuH₂ at 0.4 GPa, without significant variations. This pressure is considerably lower than the 1 GPa reported for superconductivity¹¹. These results indicate that the structure and properties of nitrogen-doped LuH₂ closely resemble those of pristine LuH₂^{13,36}.

Our comprehensive data demonstrate that nitrogen-doped LuH₂ adopts an fcc structure, undergoes pressure-induced color changes, and exhibits metallic behavior at low pressures. In stark contrast, nitrogen-doped LuH₃ retains its native trigonal lattice and lacks corresponding color changes and metallic behavior. Comparative analysis (Fig. 4a-f) reveals a striking consistency between the structure and vibrational properties of the Lu-H-N compound reported by Dasenbrock-Gammon et al. and those of fcc-structured LuH₂. This compelling evidence suggests that the reported Lu-N-H compound is LuH₂ rather than LuH₃. Furthermore, our investigation reveals minimal influence of nitrogen doping on both LuH₂ and LuH₃, further supporting this conclusion.

Nature of the reported Sharp Drop in Electrical Resistance

Across various LuH₂ samples, including nitrogen-doped, undoped, polycrystalline, and single-crystal forms, Figures 5a-c demonstrate a sharp decrease in electrical resistance with decreasing temperature. This occurs within a temperature range of 270-295 K and pressures between 1-2 GPa, without altering the crystal structures. Importantly, the transition temperature, pressure, and rate of resistance reduction align with the 294 K and 1 GPa results reported by Dasenbrock-Gammon et al. (Fig. 5d). However, zero resistance is not achieved.

Employing the background subtraction approach of Dasenbrock-Gammon et al., our data in Figures 5e-g seemingly exhibit zero resistance, hinting at potential superconductivity in line with

their study. Interestingly, around 30% of our LuH₂ samples exhibit this resistance decrease, similar to the 35% previously reported by Dasenbrock-Gammon et al. Although successful replication has been limited, the consistency of pressure and temperature conditions associated with the resistance drop across independent experiments in two different laboratories offers compelling evidence that this phenomenon reflects an electronic phase transition.

In our exploration of potential superconductivity in nitrogen-doped LuH₂, we employed Andreev reflection^{37,38} (Figures 5i-j) as a diagnostic method, in line with established protocols¹¹. This quantum mechanism enables electrons from a normal metal to pair as Cooper pairs and cross into a superconductor, typically signaling the presence of superconducting states. While Andreev reflection is prominently observable in established superconductors such as MgB₂, our experiments with nitrogen-doped LuH₂ did not reveal any distinct Andreev reflection signatures.

It is crucial to understand that the absence of clear Andreev reflection indicators does not definitively preclude the existence of superconductivity. The reliability of Andreev reflection for diagnosing superconductivity is heavily influenced by the characteristics of the tunneling barrier at the superconductor-normal metal interface. Although the lack of Andreev reflection alone does not conclusively dismiss the possibility of superconductivity, our comprehensive observations, including the absence of zero resistance, strongly imply that the reduction in electrical resistance observed in nitrogen-doped LuH₂ is not characteristic of superconducting behavior.

Previous studies have reported that mechanical grinding of polycrystalline LuH₂ at ambient conditions can lead to metal-to-insulator transitions³² and percolation³⁴—the abrupt transition from a non-conducting to a conducting state upon reaching a critical density of conductive elements. This phenomenon is typically associated with inhomogeneous systems like polycrystalline or granular materials. In contrast, our data reveal a distinct drop in electrical resistance in single-crystal LuH₂ samples within 270-295 K and 1-2 GPa. This signifies a metal-to-metal electronic transition rather than a transition to an insulator.

It is well-established that achieving true stoichiometric fcc LuH₂ is challenging. Hydrogen vacancies often form during synthesis, resulting in non-stoichiometric LuH_{2+x} compounds. These vacancies significantly impact resistivity and optical properties while leaving the overall crystal structure largely unchanged. This behavior is characteristic of rare-earth metal hydrides and has been extensively studied in materials like 'switchable mirrors'³⁹⁻⁴⁵ that switch between transparent insulating and reflective metallic states.

Therefore, the metal-to-metal electronic transition observed in our study likely arises from alterations in hydrogen-lutetium interactions influenced by factors such as pressure, strain/stress, temperature, and the spatial distribution of hydrogen vacancies. These external variables could explain the 30% -35% replication rate observed. Additionally, our investigation revealed that nitrogen doping has a negligible impact on the observed metal-to-metal transition. Encapsulating a single-crystal of LuH₂ in a nitrogen atmosphere within a diamond anvil cell at 1-2 GPa for five days resulted in no observable changes in electrical resistance.

In summary, our research refutes claims of near-ambient-condition superconductivity in nitrogen-doped LuH_{3-δ}N_ε. Data shows features attributed to LuH_{3-δ}N_ε are intrinsic to LuH₂, including the metallic fcc phase and pressure-induced color changes. We successfully replicated

the resistance drop in LuH₂ at comparable conditions with similar success rate to Dasenbrock-Gammon et al. However, our extensive investigations reveal this phenomenon to be a novel, pressure-induced metal-to-metal transition intrinsic to LuH₂, distinct from superconductivity. Additionally, nitrogen minimally impacts this transition.

Methods:

Synthesis of Lu-H-N samples. Considering that commercially available Lu metal foils often contain LuH₂ and Lu₂O₃, we used X-ray diffraction (XRD) to rigorously select the purest foils based on their diffraction patterns. All samples were handled within a glovebox and prepared with gas in a pre-purged, hydrogen-rich environment, following the procedures detailed in the original report. The conditions within the glovebox were controlled to ensure that O₂ and H₂O levels were consistently below 0.5 ppm. Subsequently, we heated the sample overnight in an oven at 65 °C, and after 24 hours, we opened a DAC to retrieve the sample.

We also used commercially available cubic LuH₂ single crystals as precursors to synthesize nitrogen-doped LuH₂. Before loading with nitrogen gas, we performed a single crystal XRD measurement to assess its quality. Several high-purity LuH₂ crystals were placed into a diamond anvil cell (DAC), loaded with nitrogen gas, and subjected to pressure increase up to 2.0 GPa. The DAC was then kept in an oven at 200 °C for 24 hours. Once the heat treatment concluded, single crystals were removed for further measurements. The synthesis process of nitrogen-doped LuH₃ was identical to that of LuH₂, using commercially available LuH₃ powders as precursors, loaded into a diamond anvil cell, pressurized to 2.0 GPa, and kept in an oven at 200 °C for 24 hours.

Single crystal and powder XRD measurements. Powder and single crystal XRD measurements were conducted on a Bruker D8 Venture diffractometer utilizing Mo K α radiation. We collected the powder XRD rings of Lu foil and LuH₃ powders, both pre- and post-heating, using a charge-coupled device detector. These data were then integrated into XRD patterns with the assistance of APEX3 software. For the high-pressure powder XRD measurements of LuH₃, both pre- and post-heating, samples were prepared in SC-type DACs with rhenium gaskets. We calibrated the distance and tilt of the detector using CeO₂ powder. For LuH₂ and nitrogen-doped LuH₂, appropriate single crystals were selected for data collection, which was conducted at room temperature. The crystal structures of LuH₂, both pre- and post-heating, were solved and refined using the APEX3 software.

Raman Spectroscopy measurements. Raman spectra of Lu, LuH₂, LuH₃, and corresponding reactants were collected using a S&I MonoVista CRS+ Raman system. The 532 nm laser was utilized for the excitation, the laser power ranges from 1.148 mW to 4.572 mW, 300 grating/mm or 2400 grating/mm was employed during the measurements. Raman system was calibrated with the single crystal silicon (520 cm⁻¹) before measurements.

High pressure electrical transport and Andreev reflections measurements. The resistance of the as-synthesized samples under high pressure was measured using the Van der Pauw method in BeCu alloy symmetric DACs with a culet size of 300 μ m. For each electrical transport measurement, a pre-pressed and drilled Re gasket insulated by *c*BN/epoxy mixtures was employed, creating a hole with a diameter of 100 μ m. Nitrogen gas and NaCl powder were used as pressure transmitting medium. Four Pt strips served as conductive wires, with ruby functioning as the pressure marker. Temperature-dependent resistance measurements were conducted on an electrical transport system, equipped with a Keithley 6221 current source, a 2182A nanovoltmeter, and a 7001 switch device. For high-pressure Andreev reflection measurements, sharp Pt tips were cut to make contact with the sample. Prior to measuring single-crystal LuH₂ in nitrogen, the Andreev reflection experiment on MgB₂ was conducted below 60 K using our electrical transport system.

Acknowledgement

We are grateful for the help from F. Liu and L. Yang for the help on the X-ray diffraction experiments. Y. Ding is also grateful for the support from the National Key Research and Development Program of China (Grant Nos. 2022YFA1402301 and 2018YFA0305703) and the National Natural Science Foundation of China (Grant Nos. U2230401). J.G. Cheng is supported by the National Key R&D Program of China (Grant No. 2021YFA1400200), the National Natural Science Foundation of China (Grant Nos. 12025408, 11921004) and the Strategic Priority Research Program of CAS (XDB33000000).

Author contributions

Y.D conceived and designed the experiments. D.W performed electrical resistance, Raman, and X-ray experiments. N.W, C.Z, C.X, W.G, X.Y, K.B, T.N, J. Z, F.G, P. D, T.M, X.L, L.S, J. C, all participated and assisted the experiments. D.W and Y.D analyzed the data. Y.D, D.W, H.M, and Q.Z discussed and interpreted the results. Y.D, D.W, and H.M wrote the paper.

Competing interest. The authors have no conflicts to disclose.

Data Availability: The data presented in this work are available upon reasonable request.

Figures

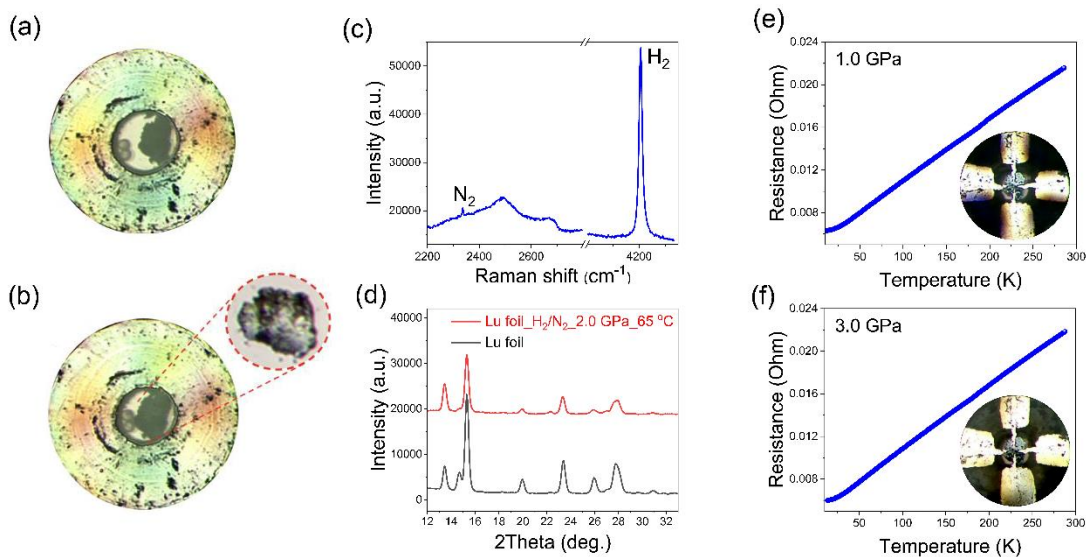


Figure 1. Synthesis and characterization of Lu metal under a $H_2:N_2$ (99:1) gas mixture following established protocol. (a) Pre-heating phase of the lutetium sample at 2.0 GPa with a 99% H_2 and 1% N_2 gas mixture at 1.0 GPa; (b) Post-heating phase for the same sample, maintained at 65 °C and 2.0 GPa for 24 hours, conspicuously devoid of the blue hue reported by Dasenbrock-Gammon et al.; (c) Raman spectrum of the gas mixture in contact with the lutetium sample; (d) X-ray diffraction (XRD) patterns for pure lutetium metal compared with the sample post 24-hour heating at 65 °C and 2.0 GPa; (e) Resistance variations with temperature for the sample post-heating at 1.0 GPa; (f) Resistance variations with temperature for the sample post-heating at 3.0 GPa.

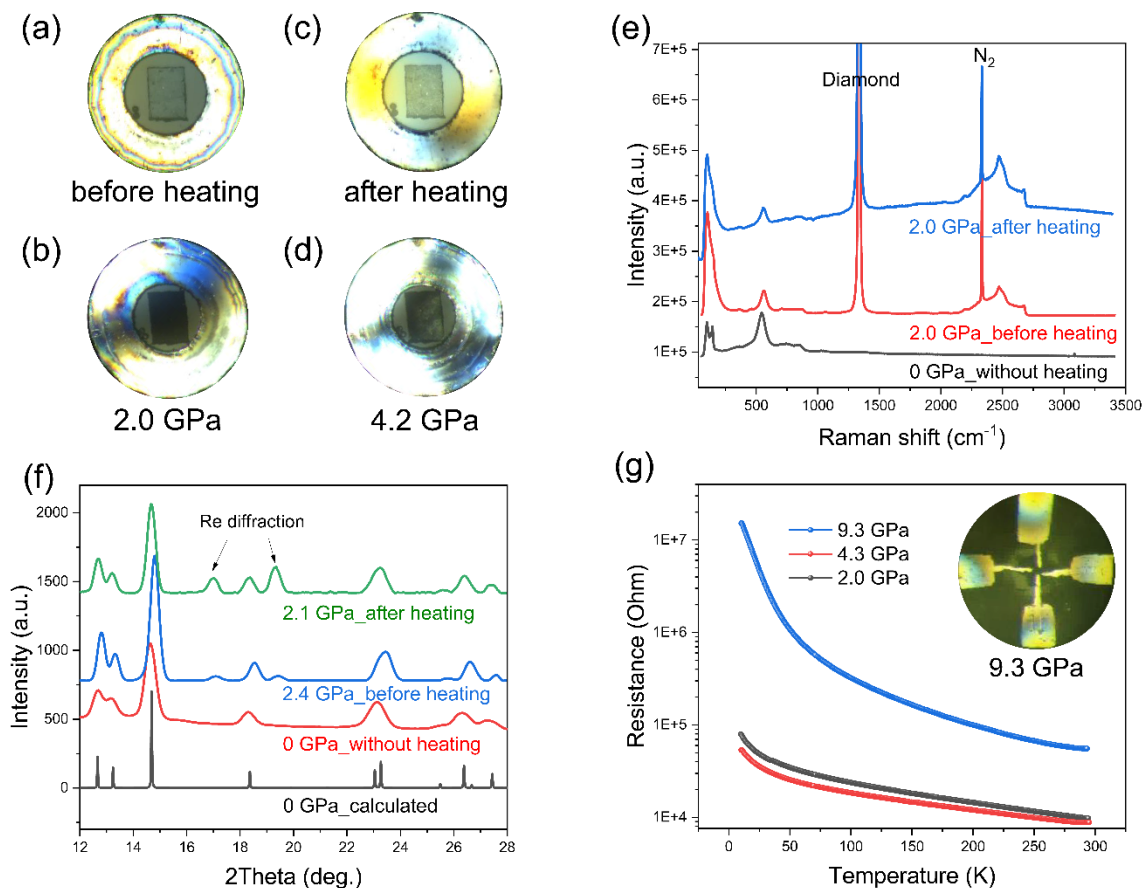


Figure 2. Characterization of nitrogen-doped LuH_3 synthesized at 200 °C and 2.0 GPa for 24 Hours. (a-d) Sequential images document the sample's color evolution during synthesis, with no observed blue-to-pink color changes. (e) Comparative Raman spectra of LuH_3 before and after pressurized heating; undoped LuH_3 spectra included for reference. (f) XRD patterns of LuH_3 pre- and post-heating, complemented by the un-doped LuH_3 pattern at 0 GPa and a simulated LuH_3 pattern. (g) Resistance as a function of temperature for nitrogen-doped LuH_3 at pressures from 2.0 GPa to 9.3 GPa. The inset illustrates the four-probe measurement.

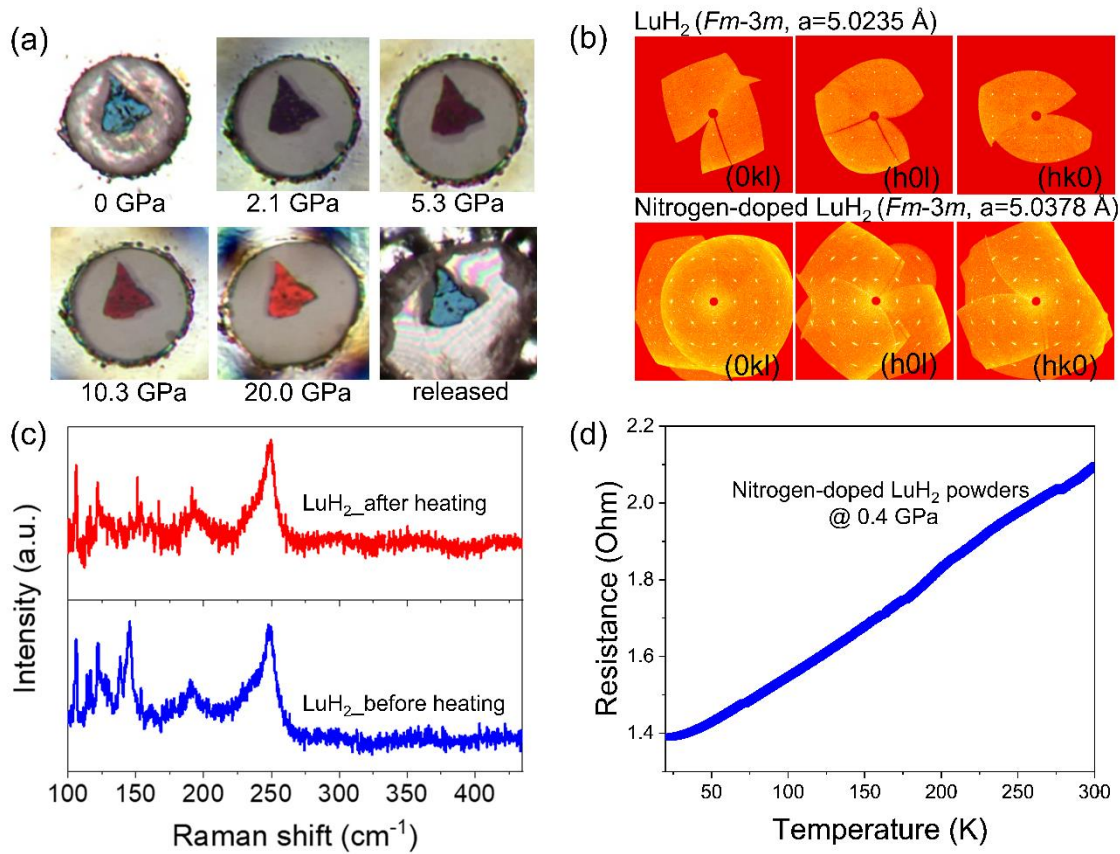


Figure 3. Characterization of nitrogen-doped LuH₂ produced from single-crystal LuH₂ treated in N₂ gas at 200 °C and 2.0 GPa. (a) Sequential photographs capture the sample's color evolution as pressure ranges from 0 to 20.0 GPa. (b) XRD patterns of both un-doped and nitrogen-doped LuH₂ single-crystals. (c) Raman spectra of LuH₂ pre- and post-heat treatment. (d) Electrical transport behavior of nitrogen-doped LuH₂ powders under 0.4 GPa.

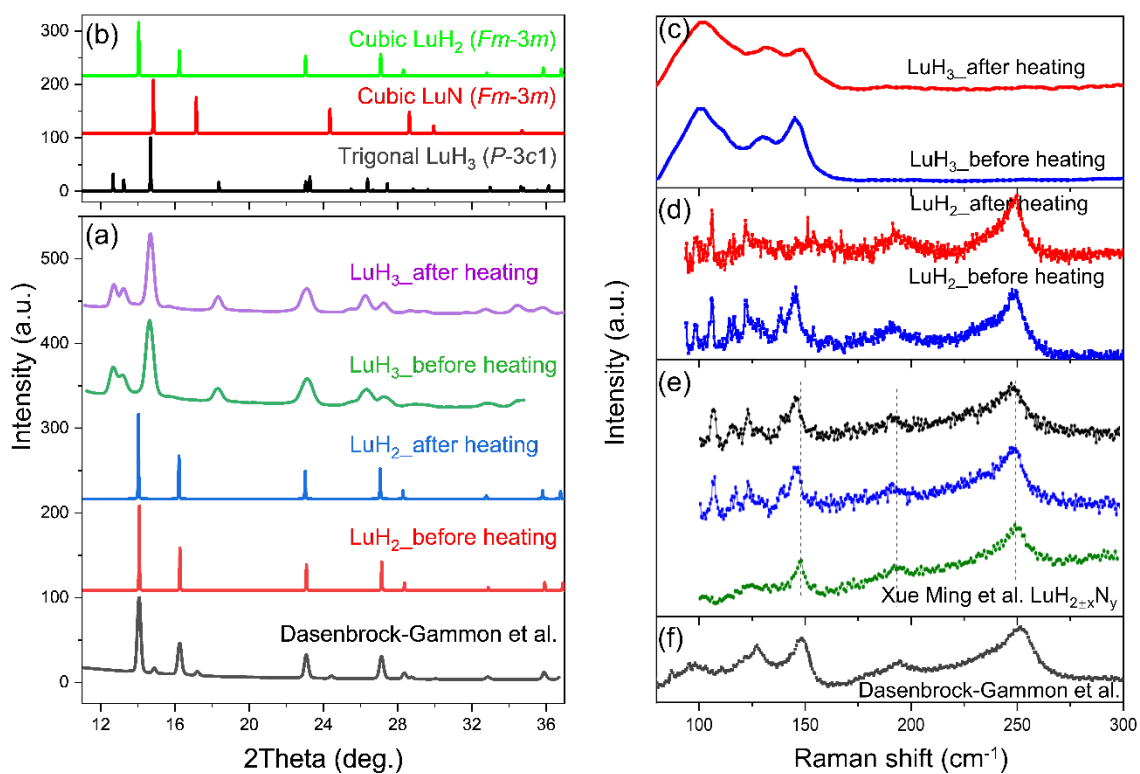


Figure 4. Detailed comparison of structure and properties of LuH₂ and LuH₃. (a) The XRD patterns of LuH₂ and LuH₃ before and after heating, along with the diffraction pattern of the Lu-N-H compound; (b) The simulated XRD pattern of LuH₂ (*Fm-3m*), LuN (*Fm-3m*), and LuH₃ (*P-3c1*); (c) Raman spectra of LuH₃ before and after heating; (d) Raman spectrum of LuH₂ before and after heating; (e) Raman spectra of as-synthesized LuH_{2-x}N_y compounds from Xue Ming et al.¹⁸; (f) Raman spectrum of the Lu-H-N compound¹¹.

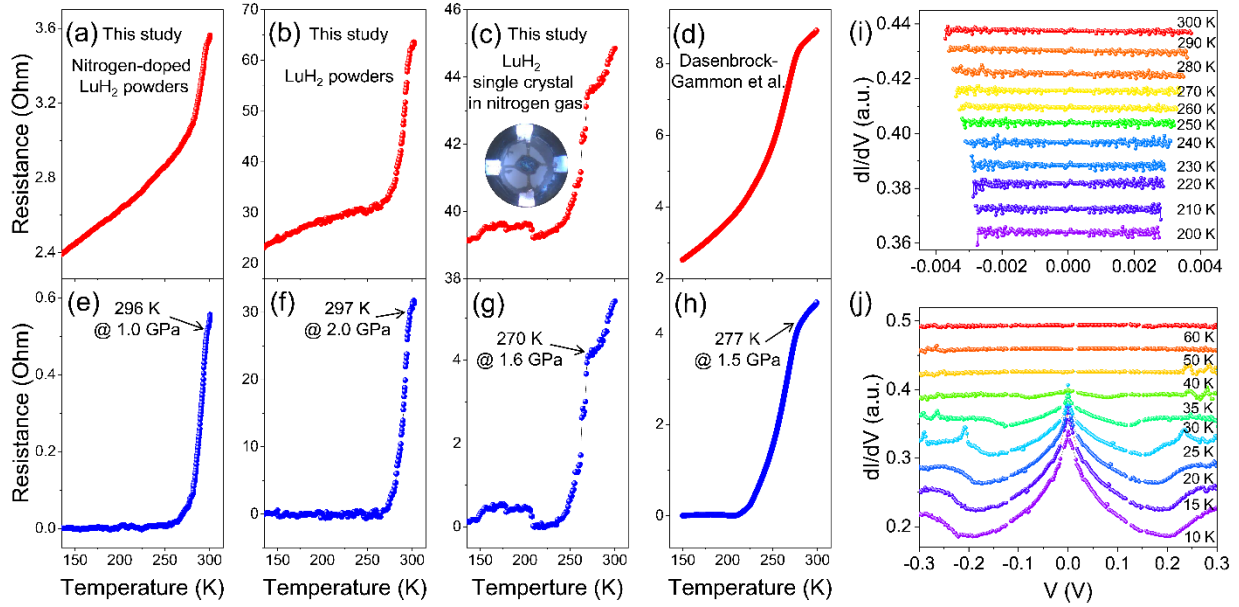


Figure 5. Comparative electrical resistance measurements of nitrogen-doped and pristine LuH₂ in various forms and under pressures in range of 1-2 GPa. (a) Electrical resistance of nitrogen-doped, polycrystalline LuH₂, illustrating a drop at 296 K and 1.0 GPa; (b) Electrical resistance of pristine, polycrystalline LuH₂, showing a drop at 297 K and 2.0 GPa; (c) Electrical resistance of single-crystal LuH₂ in a nitrogen gas, indicating a drop at 270 K and 1.6 GPa. Inset: Optical photograph of the four-probe electrical resistance setup in a diamond anvil cell; (d) Data from Dasenbrock-Gammon et al., exhibiting a resistance drop at 296 K and 1.0 GPa; (e)-(h) Resistance profiles after background subtraction, following the methodology of Dasenbrock-Gammon et al.; (i) Andreev reflection measurements from single-crystal LuH₂ under 1.6 GPa in nitrogen; (j) Andreev reflection measurements from standard MgB₂ for comparison, conducted under identical experimental conditions.

Supplementary materials

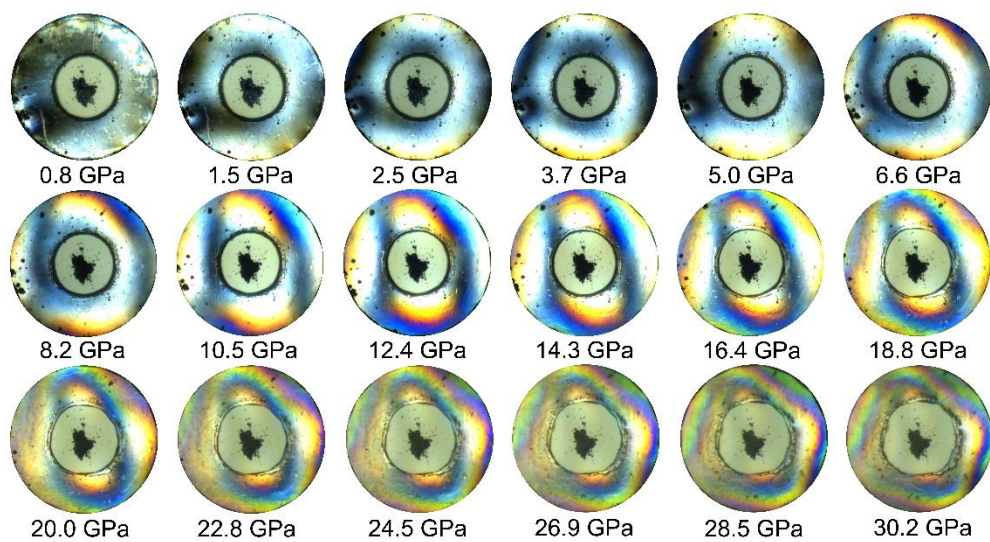


Figure S1. Pressure-dependent color changes of nitrogen-doped LuH₃.

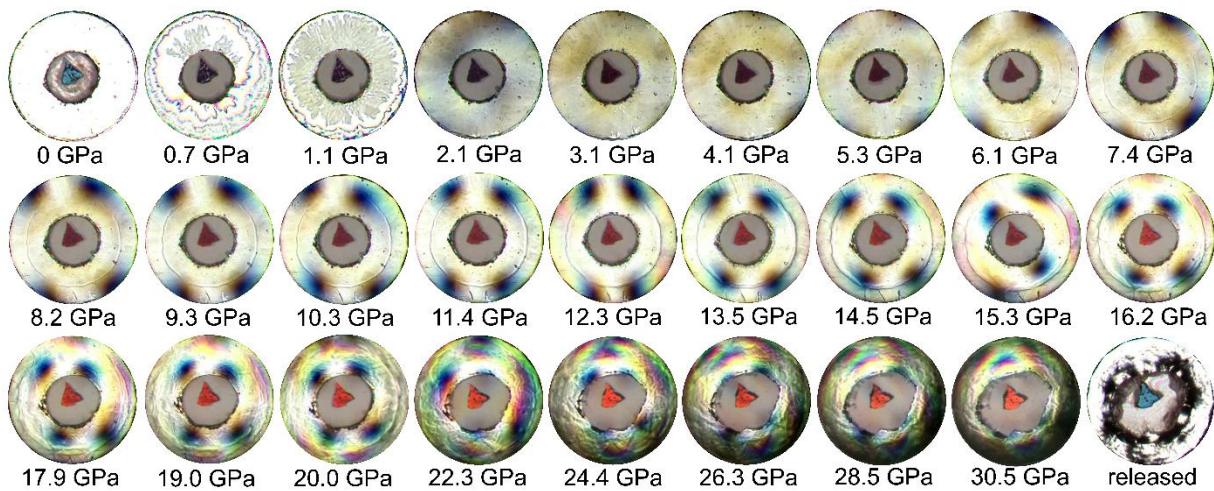


Figure S2. Pressure-dependent color changes of nitrogen-doped LuH₂.

References

- 1 Onnes, H. K. The superconductivity of mercury. *Comm. Phys. Lab. Univ. Leiden* **122**, 124 (1911).
- 2 Gao, L., Xue, Y., Chen, F., Xiong, Q., Meng, R. *et al.* Superconductivity up to 164 K in $\text{HgBa}_2\text{Ca}_m\text{-iCu}_m\text{O}_{2m+2+\delta}$ ($m=1, 2$, and 3) under quasihydrostatic pressures. *Physical Review B* **50**, 4260 (1994).
- 3 Schilling, A., Cantoni, M., Guo, J. & Ott, H. Superconductivity above 130 K in the Hg–Ba–Ca–Cu–O system. *Nature* **363**, 56-58 (1993).
- 4 Pickard, C. J., Errea, I. & Eremets, M. I. Superconducting hydrides under pressure. *Annual Review of Condensed Matter Physics* **11**, 57-76 (2020).
- 5 Drozdov, A., Eremets, M., Troyan, I., Ksenofontov, V. & Shylin, S. I. Conventional superconductivity at 203 kelvin at high pressures in the sulfur hydride system. *Nature* **525**, 73-76 (2015).
- 6 Somayazulu, M., Ahart, M., Mishra, A. K., Geballe, Z. M., Baldini, M. *et al.* Evidence for superconductivity above 260 K in lanthanum superhydride at megabar pressures. *Physical Review Letters* **122**, 027001 (2019).
- 7 Wang, D., Ding, Y. & Mao, H.-K. Future study of dense superconducting hydrides at high pressure. *Materials* **14**, 7563 (2021).
- 8 Bi, J., Nakamoto, Y., Zhang, P., Shimizu, K., Zou, B. *et al.* Giant enhancement of superconducting critical temperature in substitutional alloy (La, Ce) H_9 . *Nature Communications* **13**, 5952 (2022).
- 9 Ma, L., Wang, K., Xie, Y., Yang, X., Wang, Y. *et al.* High-temperature superconducting phase in clathrate calcium hydride CaH_6 up to 215 K at a pressure of 172 GPa. *Physical Review Letters* **128**, 167001 (2022).
- 10 Kong, P., Minkov, V. S., Kuzovnikov, M. A., Drozdov, A. P., Besedin, S. P. *et al.* Superconductivity up to 243 K in the yttrium-hydrogen system under high pressure. *Nature communications* **12**, 5075 (2021).
- 11 Dasenbrock-Gammon, N., Snider, E., McBride, R., Pasan, H., Durkee, D. *et al.* Evidence of near-ambient superconductivity in a N-doped lutetium hydride. *Nature* **615**, 244-250 (2023).
- 12 Dasenbrock-Gammon, N., Snider, E., McBride, R., Pasan, H., Durkee, D. *et al.* Retraction Note: Evidence of near-ambient superconductivity in a N-doped lutetium hydride. *Nature* **624**, 460-460, doi:10.1038/s41586-023-06774-2 (2023).
- 13 Shan, P., Wang, N., Zheng, X., Qiu, Q., Peng, Y. *et al.* Pressure-induced color change in the lutetium dihydride LuH_2 . *Chinese Physics Letters* **40**, 046101 (2023).
- 14 Liu, Z., Zhang, Y., Huang, S., Ming, X., Li, Q. *et al.* Pressure-induced color change arising from transformation between intra- and inter-band transitions in $\text{LuH}_{2\pm x}\text{N}_y$. *Science China Physics, Mechanics & Astronomy* **67**, 227411, doi:10.1007/s11433-023-2222-3 (2024).
- 15 Zhang, Y.-J., Ming, X., Li, Q., Zhu, X., Zheng, B. *et al.* Pressure induced color change and evolution of metallic behavior in nitrogen-doped lutetium hydride. *Science China Physics, Mechanics & Astronomy* **66**, 287411 (2023).
- 16 Lv, R., Tu, W., Shao, D., Sun, Y. & Lu, W. Physical Origin of Color Changes in Lutetium Hydride under Pressure. *Chinese Physics Letters* **40**, 117401, doi:10.1088/0256-307X/40/11/117401 (2023).
- 17 Xing, X., Wang, C., Yu, L., Xu, J., Zhang, C. *et al.* Observation of non-superconducting phase changes in nitrogen doped lutetium hydrides. *Nature Communications* **14**, 5991 (2023).
- 18 Ming, X., Zhang, Y.-J., Zhu, X., Li, Q., He, C. *et al.* Absence of near-ambient superconductivity in $\text{LuH}_{2\pm x}\text{N}_y$. *Nature*, 1-3 (2023).

- 19 Tao, X., Yang, A., Yang, S., Quan, Y. & Zhang, P. Leading components and pressure-induced color changes in N-doped lutetium hydride. *Science Bulletin* **68**, 1372-1378, doi:<https://doi.org/10.1016/j.scib.2023.06.007> (2023).
- 20 Kim, S.-W., Conway, L. J., Pickard, C. J., Pascut, G. L. & Monserrat, B. Microscopic theory of colour in lutetium hydride. *arXiv preprint arXiv:2304.07326* (2023).
- 21 Zhao, X., Shan, P., Wang, N., Li, Y., Xu, Y. *et al.* Pressure tuning of optical reflectivity in LuH₂. *Science Bulletin* **68**, 883-886, doi:<https://doi.org/10.1016/j.scib.2023.04.009> (2023).
- 22 Dangić, Đ., Garcia-Goiricelaya, P., Fang, Y.-W., Ibañez-Azpiroz, J. & Errea, I. Ab initio study of the structural, vibrational, and optical properties of potential parent structures of nitrogen-doped lutetium hydride. *Physical Review B* **108**, 064517 (2023).
- 23 Pavlov, N. S., Shein, I. R., Pervakov, K. S., Pudalov, V. M. & Nekrasov, I. A. Anatomy of the band structure of the newest apparent near-ambient superconductor LuH_{3-x}N_x. *arXiv preprint arXiv:2306.09868* (2023).
- 24 Tresca, C., Forcella, P. M., Angeletti, A., Ranalli, L., Franchini, C. *et al.* Evidence of molecular hydrogen in the N-doped LuH₃ system: a possible path to superconductivity? *arXiv preprint arXiv:2308.03619* (2023).
- 25 Huo, Z., Duan, D., Ma, T., Jiang, Q., Zhang, Z. *et al.* First-principles study on the superconductivity of N-doped fcc-LuH₃. *arXiv preprint arXiv:2303.12575* (2023).
- 26 Denchfield, A., Park, H. & Hemley, R. J. Novel electronic structure of nitrogen-doped lutetium hydrides. *arXiv preprint arXiv:2305.18196* (2023).
- 27 Ferreira, P. P., Conway, L. J., Cucciari, A., Di Cataldo, S., Giannessi, F. *et al.* Search for ambient superconductivity in the Lu-N-H system. *Nature Communications* **14**, 5367, doi:10.1038/s41467-023-41005-2 (2023).
- 28 Lucrezi, R., Ferreira, P. P., Aichhorn, M. & Heil, C. Temperature and quantum anharmonic lattice effects on stability and superconductivity in lutetium trihydride. *Nature Communications* **15**, 441, doi:10.1038/s41467-023-44326-4 (2024).
- 29 Moulding, O., Gallego-Parra, S., Gao, Y., Toulemonde, P., Garbarino, G. *et al.* Pressure-induced formation of cubic lutetium hydrides derived from trigonal LuH₃. *Physical Review B* **108**, 214505, doi:10.1103/PhysRevB.108.214505 (2023).
- 30 Tkacz, M. & Palasyuk, T. Pressure induced phase transformation of REH₃. *Journal of Alloys and Compounds* **446-447**, 593-597, doi:<https://doi.org/10.1016/j.jallcom.2006.11.042> (2007).
- 31 Hirsch, J. Enormous variation in homogeneity and other anomalous features of room temperature superconductor samples: A comment on Nature 615, 244 (2023). *Journal of Superconductivity and Novel Magnetism*, 1-6 (2023).
- 32 Peng, D., Zeng, Q., Lan, F., Xing, Z., Ding, Y. *et al.* The near-room-temperature upsurge of electrical resistivity in Lu-HN is not superconductivity, but a metal-to-poor-conductor transition. *Matter and Radiation at Extremes* **8** (2023).
- 33 Cai, S., Guo, J., Shu, H., Yang, L., Wang, P. *et al.* No evidence of superconductivity in a compressed sample prepared from lutetium foil and H₂/N₂ gas mixture. *Matter and Radiation at Extremes* **8** (2023).
- 34 Wang, N., Hou, J., Liu, Z., Lu, T., Shan, P. *et al.* Percolation-induced resistivity drop in lutetium dihydride with controllable electrical conductivity over six orders of magnitude. *Science China Physics, Mechanics & Astronomy* **66**, 297412 (2023).

- 35 Mao, H.-K., Chen, X.-J., Ding, Y., Li, B. & Wang, L. Solids, liquids, and gases under high pressure. *Reviews of Modern Physics* **90**, 015007, doi:10.1103/RevModPhys.90.015007 (2018).
- 36 Li, P., Bi, J., Zhang, S., Cai, R., Su, G. *et al.* Transformation of hexagonal Lu to cubic LuH_{2+x} single-crystalline films. *arXiv preprint arXiv:2304.07966* (2023).
- 37 Andreev, A. The thermal conductivity of the intermediate state in superconductors. *Журнал экспериментальной и теоретической физики* **46**, 1823-1828 (1964).
- 38 Cao, Z.-Y., Jang, H., Choi, S., Kim, J., Kim, S. *et al.* Spectroscopic evidence for the superconductivity of elemental metal Y under pressure. *NPG Asia Materials* **15**, 5, doi:10.1038/s41427-022-00457-6 (2023).
- 39 Palm, K. J., Murray, J. B., Narayan, T. C. & Munday, J. N. Dynamic optical properties of metal hydrides. *ACS Photonics* **5**, 4677-4686 (2018).
- 40 Ng, K., Zhang, F., Anisimov, V. & Rice, T. Electronic structure of lanthanum hydrides with switchable optical properties. *Physical Review Letters* **78**, 1311 (1997).
- 41 Van Gogh, A., Kooij, E. S. & Griessen, R. Isotope effects in switchable metal-hydride mirrors. *Physical Review Letters* **83**, 4614 (1999).
- 42 Ng, K., Zhang, F., Anisimov, V. & Rice, T. Theory for metal hydrides with switchable optical properties. *Physical Review B* **59**, 5398 (1999).
- 43 Remhof, A. & Borgschulte, A. Thin-film metal hydrides. *Chemphyschem* **9**, 2440-2455, doi:10.1002/cphc.200800573 (2008).
- 44 Den Broeder, F., Van der Molen, S., Kremers, M., Huiberts, J., Nagengast, D. *et al.* Visualization of hydrogen migration in solids using switchable mirrors. *Nature* **394**, 656-658 (1998).
- 45 Huiberts, J. N., Griessen, R., Rector, J., Wijngaarden, R., Dekker, J. *et al.* Yttrium and lanthanum hydride films with switchable optical properties. *Nature* **380**, 231-234 (1996).